The 6th International Supercritical CO_2 Power Cycles Symposium
March 27 - 29, 2018, Pittsburgh, Pennsylvania

A preliminary comparison of different turbine architectures for a 100 kW supercritical CO_2 Rankine cycle turbine

Martin T. White
Research Associate
Department of Mechanical Engineering and Aeronautics
City, University of London
Northampton Square,
London, UK, EC1V 0HB
martin.white@city.ac.uk

Abdulnaser I. Sayma
Professor of Energy Engineering
Department of Mechanical Engineering and Aeronautics
City, University of London
Northampton Square,
London, UK, EC1V 0HB
a.sayma@city.ac.uk

ABSTRACT

The aim of this paper is to conduct a preliminary comparison of different turbine architectures for a small-scale 100 kW supercritical CO_2 Rankine cycle. The turbine is required to expand supercritical CO_2 from 650 °C and 170 bar, down to 50 bar. For such an application, it is not immediately clear which turbine architecture is the most suitable design when considering both aerodynamic and mechanical design constraints. Within this paper, three different turbine architectures are considered, namely radial-inflow, single-stage axial, and two-stage axial turbines. For each architecture, a preliminary design model is constructed which is based on conventional turbomachinery design parameters such as the loading coefficient, flow coefficient and degree of reaction. Using this model, a parametric investigation on the effect of the rotational speed on the required rotor diameter and blade height is conducted and the different turbine architectures are compared. This is completed with the view of establishing the feasible design space for a small-scale supercritical CO_2 turbine. For all three architectures, it is found that in order to obtain feasible blade heights it is necessary to maximise the loading coefficient whilst minimising the flow coefficient, and design the turbine with the minimum allowable diameter. Typically, this results in a turbine design with a rotor diameter of 30 mm, a rotor-inlet blade height in the range of 1.74 to 2.47 mm, and a rotational speed between 150 and 250 kRPM for a single-stage radial or axial turbine, and 75 and 175 kRPM for a two-stage axial turbine. Ultimately, nine candidate turbine designs have been identified, which should be studied further using more advanced 3D CFD and FEA simulations.

INTRODUCTION

In the past decade, the search for the next generation of high-efficiency thermal power cycles has led to a significant interest in supercritical carbon dioxide (sCO_2) as a working fluid. One of the primary benefits in operating a thermodynamic cycle with sCO_2 is that high efficiency can be obtained at moderate turbine inlet temperatures (in the region of 500 °C), which makes sCO_2 an interesting option for applications such as nuclear power [1], concentrated-solar power [2] and high efficiency coal-fired power plants [3]. Moreover, sCO_2 cycles can also be considered for waste-heat recovery applications for heat-source temperatures exceeding 450 °C [4]; at this temperature, organic Rankine cycles, which would typically be considered for waste-heat recovery, are not suitable due to factors such as fluid decomposition and low efficiency, whilst sCO_2 have the advantage of compactness and simplicity compared to steam Rankine cycles. At present, the primary focus of sCO_2 research and development activities has been on medium- to large-scale applications, with power outputs in the order of 1 MW_e and above, for example in Refs. [5,6]. However, given the potential thermodynamic benefits, sCO_2 cycles can also be considered for small-scale applications with power outputs in the order of 100 kW_e, and systems of this size are already under investigation [7-9].

As recently discussed in Ref. [10], there are a large number of variants of sCO_2 cycle, and each variant has a varying degree of complexity. However, for a small-scale application a simple recuperated cycle, comprising of compressor/pump, heat-addition heat exchanger, turbine, recuperator and heat-rejection heat exchanger, is probably the most suitable cycle based on both cost and technical considerations. Depending on the inlet conditions to the compression process this simple recuperated cycle can either operate as a Rankine cycle or a Brayton cycle. The effect of the compression inlet temperature T_c, and compression inlet pressure p_c, on the operating condition and performance of a sCO2 cycle is shown in Fig. 1. As observed from the analysis shown in Fig. 1, operating with a low inlet temperature to the compression process corresponds to operating a Rankine cycle, and this can achieve a higher thermal efficiency than the Brayton cycle operating under the same assumptions. Therefore, operating a Rankine cycle is preferential from a thermodynamic perspective. However, since the critical temperature of CO_2 is 31 °C, it is only possible to operate a sCO_2 Rankine cycle in areas with a low ambient temperature. However, there has been recent research into mixing CO_2 with small amounts of other fluids to obtain a CO_2 blend that has a higher pseudo-critical temperature [11,12]. Using a blend could therefore realise the potential of the sCO_2 Rankine cycle in areas with higher ambient temperatures.

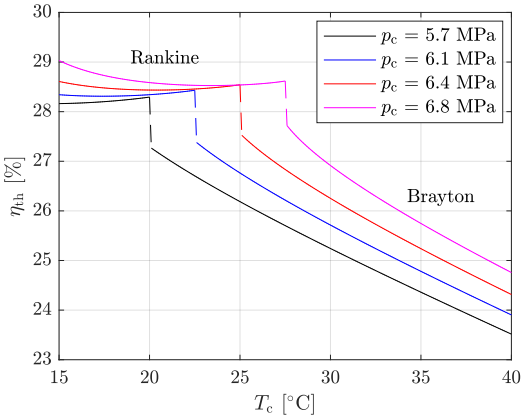

Figure 1. Effect of the inlet conditions of the compression process (inlet temperature T_c, and inlet pressure p_c) on the thermal efficiency of a sCO_2 cycle, assuming a turbine inlet temperature of T_{01} = 650 °C, pressure ratio of PR = 3, compression and expansion isentropic efficiencies of $\eta_{c,is}$ = 0.7 and $\eta_{t,is}$ = 0.8 respectively, and a recuperator effectiveness of ϵ_r = 0.8.

Another advantage of sCO_2 is that it has a high density, which facilitates the miniaturisation of system components, enabling a high power density compared to conventional power plants. Whilst this is advantageous from the point of view of reducing the size, and cost of the plant, it presents challenges with regards to turbomachinery design. More specifically, to achieve a high efficiency the turbomachinery components become very small and must rotate at high speed. This results in low aspect-ratio blades (blade height to chord ratio), and increased relative clearance gaps, which give rise to increased secondary flow and over the tip gap losses. Furthermore, the combined effects of a high power density, high operating pressures, high rotational speeds and small component dimensions mean that the design of the bearing-shaft arrangement needs to be carefully considered, in addition to considering the axial thrust that is exerted by the rotor on the bearings. Moreover, for the relatively low pressure-ratio and mass-flow rate, it is not immediately obvious weather a radial-inflow or axial-flow turbine is the most suitable design when considering both aerodynamic and mechanical design constraints.

The aim of this paper is to conduct a preliminary comparison of different turbine architectures for a small-scale sCO_2 Rankine cycle system, and establish the feasible design space for different turbine types. Focus is given here on the turbine based on the premise that the future use of CO_2-blends could realise the potential to operate a Rankine cycle, thus removing the need for a compressor.

THERMODYNAMIC SPECIFICATION AND PRELIMINARY TURBINE SIZING

The results from a thermodynamic analysis of a recuperated sCO_2 Rankine cycle are shown in Fig. 2. For

this analysis, a compressor inlet temperature of 20 °C is assumed, and the effect of the turbine inlet temperature T_{01} and pressure ratio PR on the thermal efficiency η_{th} and turbine inlet pressure p_{01} has been investigated. These calculations have been completed assuming fixed polytropic efficiencies of 70% and 80% for the pump and turbine respectively, and a recuperator effectiveness of 80%.

It is observed from Fig. 2 that as PR increases, η_{th} increases, but at the expense of higher operating pressures. For T_{01} = 650 °C, PR = 3 has been selected as this is considered to be reasonable compromise, corresponding to η_{th} = 28%, and p_{01} = 17 MPa. The turbine design specification is summarised in Table 1.

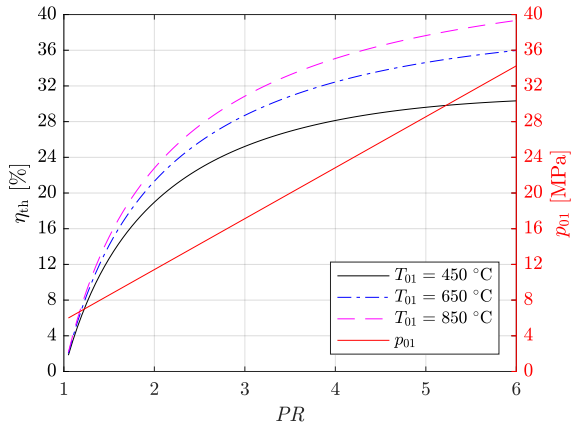

Figure 2. Effect of pressure ratio PR and turbine inlet temperature T_{01} on thermal efficiency η_{th} and turbine inlet pressure p_{01} of a recuperatred sCO_2 Rankine cycle (T_{c}= 20 °C, $\eta_{\mathrm{c,p}}$ = 0.7, $\eta_{\mathrm{t,p}}$ = 0.8, ϵ_{r} = 0.8).

Table 1. Design specification of the sCO_2 turbine.

T_{01}	650	°C
p_{01}	17.0	MPa
PR	3	-
$\dot{m}$	0.65	kg/s
$\dot{W}$	100	kW
$\eta_{\mathrm{t,is}}$ (target)	0.8	-

Based on the information provided in Tab. 1 a preliminary assessment of a single-stage turbine, either radial-inflow or axial-flow, can be completed using the specific speed ω_{s}:

$$\omega_{\mathrm{s}} = \frac{\omega \dot{V}_3^{\frac{1}{2}}}{\Delta h_{\mathrm{ss}}}\,, \tag{1}$$

where ω is the rotor rotational speed in rad/s, $\dot{V}_3$ is the volumetric flow rate at the rotor outlet in m^3/s and Δh_{ss} is the isentropic enthalpy drop across the expander, given in J/kg. In general, optimal turbine efficiency occurs within a certain range of values for ω_{s}, typically $0.1 < \omega_{\mathrm{s}} < 1.0$ [13] (Fig. 3a), and therefore ω can be found by rearranging Equation 1. This calculation can be completed using the information provided in Tab. 1, if the total and static conditions at the rotor outlet are assumed equal.

For a two-stage turbine Equation 1 is still valid, but instead applies to each individual stage. In this case the total enthalpy drop across the entire turbine is equally divided across the two stages, and each stage is assumed to operate with the same isentropic efficiency (*i.e.*, $\eta_{\mathrm{t,is}}$= 80%). It is assumed that both stages are mounted on the same shaft, and therefore both stages rotate at the same speed. Therefore, the second stage will have a higher specific speed than the first, owing to the lower density. In this instance, the quoted value for ω_{s} refers to the first stage only. For the case study in question, the specific speed of stage two is then 27% higher than stage one. For a first-stage specific speed below 0.5, the second-stage specific speed will therefore be below 0.64. Therefore, since this is still within the limits previously stated, a penalty in the second-stage efficiency is not expected.

The required rotational speed (in kRPM) for a single- and two-stage turbine for ω_{s} ranging between 0.05 and 0.6 is shown in Fig. 3b. For a single-stage turbine to operate at an optimal efficiency, the rotor must rotate at a speed in the region of a few-hundred kRPM, which introduces challenges with regards to the mechanical and electrical design of the turbine. Reducing the speed could simplify these aspects, but at the penalty of a reduced aerodynamic efficiency. Comparatively, a two-stage design facilitates a higher

specific speed to be obtained at a lower rotational speed, but at the complexity of requiring multiple stages. Clearly, a trade-off exists between aerodynamic performance, and mechanical/electrical constraints.

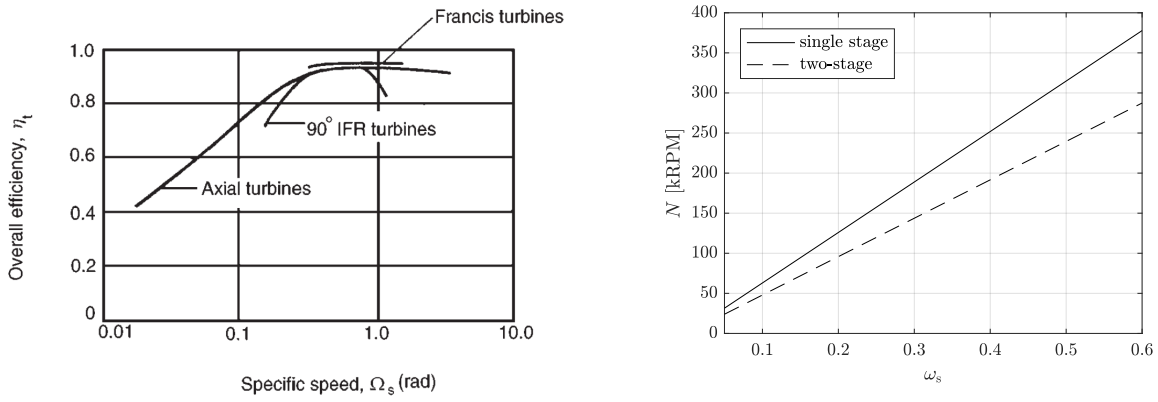

(a) (b)

Figure 3. (a) Effect of specific speed on turbine efficiency for different turbine types, taken from Ref. [13]; (b) the required rotational speed for a single- and two-stage turbine as a function of the desired rotor specific speed ω_s. For the two-stage turbine, ω_s refers to the specific speed of the first stage.

RADIAL TURBINE DESIGN

To obtain a preliminary radial-turbine design, a design model has been developed, which is coupled to NIST REFPROP [14] to obtain the thermodynamic properties of CO_2. The selected design parameters are the rotational speed N, blade-loading coefficient Ψ, and flow coefficient Φ, which are defined as:

$$\Psi = \frac{\Delta h_0}{u_2^2} \; ; \tag{2}$$

$$\Phi = \frac{c_{\mathrm{m3}}}{u_2} , \tag{3}$$

where Δh_0 is the total enthalpy drop across the turbine, u_2 is the rotor-inlet blade velocity and c_{m3} is the meridional velocity at the rotor outlet. Using the defined target efficiency, the total enthalpy drop across the turbine can be determined since $\Delta h_0 = \eta_{\mathrm{t,is}} \Delta h_{\mathrm{ss}}$, from which u_2 follows. Moreover, although a small amount swirl at the rotor outlet is often applied in practice, for simplicity the rotor outlet is designed for zero swirl. Therefore, the absolute tangential velocity at the rotor inlet $c_{\theta 2}$ can be determined since the stage enthalpy drop reduces to $\Delta h_0 = u_2 c_{\theta 2}$. Then, assuming a constant meridional velocity (*i.e.*, $c_{\mathrm{m3}} = c_{\mathrm{m3}}$), the rotor inlet velocity triangle is fully defined. Finally, if a loss coefficient is applied to account for losses within the stator, the density at the rotor inlet and, in turn, the rotor-inlet dimensions (*i.e.*, blade height b_2, and diameter d_2) are found.

To design the rotor outlet an additional design parameter must be defined. However, at this stage of the design process it is not clear whether a 90° radial-inflow turbine, a radial-inflow turbine with a non-zero inlet blade angle, or even a highly-loaded impulse-type turbine would be the most suitable choice. However, since the rotor-inlet design is a function of only N, Ψ and Φ, and is therefore independent of the rotor-outlet design, a parametric investigation concerning these three parameters can be conducted. For this investigation constraints were placed on the minimum allowable rotor diameter ($d_2 \geq 30$ mm), maximum rotor-inlet absolute flow angle ($\alpha_2 \leq 82.5°$), and minimum allowable blade height ($b_2 \geq 1.25$ mm). Of these constraints, the rotor-inlet blade height is expected to be the most significant, owing to the relative size of clearance gaps, and values in the region of 1 to 2 mm are currently considered to be close to the limit of practicality [15,16]. Alongside these constraints, a stator loss coefficient of $\zeta_{\mathrm{n}} = 0.075$ is assumed. Fixing ζ_{n} means there is no consideration of the effect that changing the rotor-inlet velocity has on the stator performance, however this is not expected to have a significant effect on the final rotor-inlet dimensions.

Results for three rotational speeds, namely 150, 200 and 250 kRPM, are shown in Fig. 4. These three

speeds correspond to specific speeds of 0.24, 0.32 and 0.40 respectively. The analysis was also conducted for 100 and 300 kRPM, however no design could be found that met all of the imposed constraints. In general, it is observed that increasing Ψ corresponds to a reduction in d_2, but an increase in b_2. Moreover, for a specified Ψ, reducing Φ increases b_2 further, but at the cost of increasing α_2. Ultimately, the result of this interplay between the design parameters and constraints means that in order to maximise the blade height, it is necessary to design a turbine with small diameter, and a high absolute flow angle.

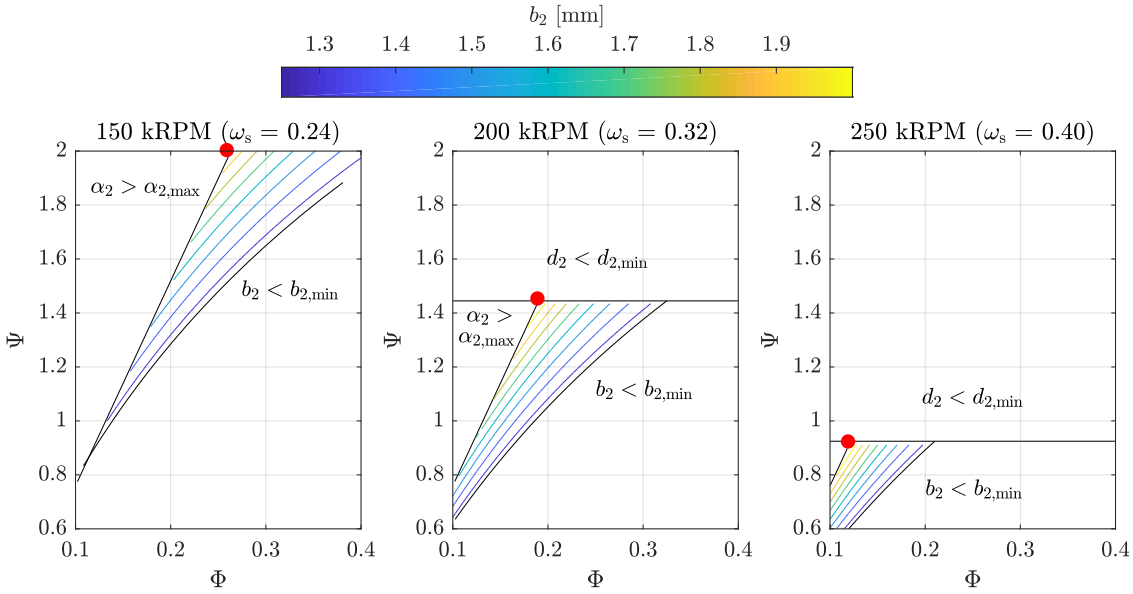

Figure 4. Effect of rotational speed, blade-loading coefficient Ψ, and flow coefficient Φ on the rotor-inlet blade height of a radial-inflow turbine. The red dots correspond to the designs summarised in Tab. 2.

For each rotational speed, the designs that maximise b_2 are summarised in Tab. 2, and these designs are shown by the red dots in Fig. 4. The velocity triangles for these designs are presented in Fig. 5. From these results, it is observed that a different type of radial-inflow turbine is required as the rotational speed is reduced. At 250 kRPM the blade-loading coefficient is below unity, implying a 90° radial-inflow turbine design. In order to maximise the blade height (b_2= 2.13 mm), a flow coefficient of 0.12 is required, corresponding to α_2= 82.5°, and a relative flow angle of β_2= -31.7°, which is within the recommended range of -40° to -20° [13]. Increasing Φ to 0.16, reduces α_2 by 2.5°, and the b_2 to 1.60 mm. On the other hand, increasing the diameter to 35 mm, increases β_2 to -74.4°, which is no longer within the recommended limits.

As the speed is reduced to 200 kRPM, it is necessary to have a blade-loading coefficient above unity, and therefore a rotor with a non-zero rotor inlet blade angle is required. Then, as the rotational speed is further reduced to 150 kRPM, a high blade-stage loading coefficient, approaching 2, is required to obtain a blade height close to 2 mm. This implies a highly-loaded rotor, with a degree of reaction approaching zero. In this case, the rotor is an impulse turbine, with the majority of the expansion occurring in the stator. It is also noted that for the 150 kRPM design, the feasible design space is not constrained by the minimum diameter (30 mm), hence the design that maximises the blade height has a slightly larger diameter.

Table 2. Summary of radial turbine rotor design that maximises the rotor-inlet blade height for the three different rotational speeds considered.

	N [kRPM]	Ψ	Φ	d_2 [mm]	b_2 [mm]	α_2 [°]	β_2 [°]	Ma_2	Rotor type
Radial 1	150	2.00	0.26	34.00	1.98	82.50	75.25	1.25	Impulse
Radial 2	200	1.45	0.19	30.00	2.09	82.50	66.85	1.03	Backswept
Radial 3	250	0.92	0.12	30.00	2.13	82.50	–31.74	0.81	90° IFR

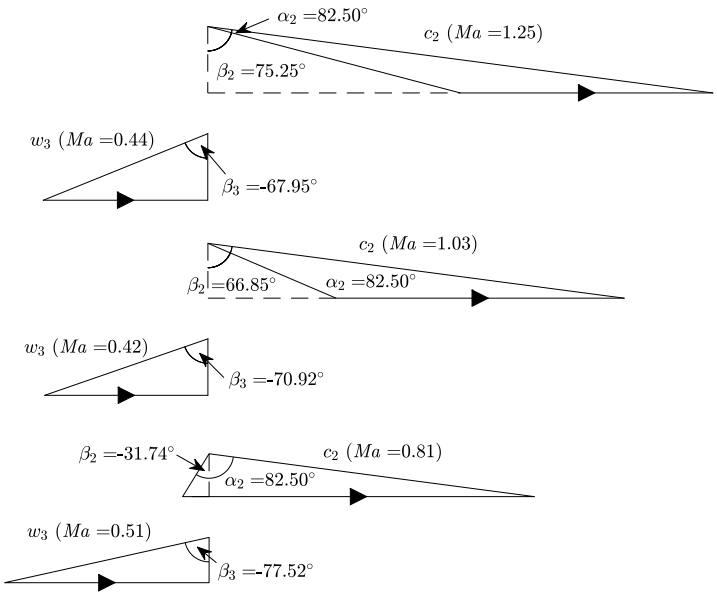

Figure 5. Velocity triangles for the three radial-turbine rotor designs given in Tab. 2. From top to bottom: design 1 (150 kRPM); design 2 (200 kRPM); design 3 (250 kRPM). The rotor-outlet velocity triangles are obtained by assuming rotor diameter ratios (d_3/d_2) of 0.65, 0.55 and 0.55 for design 1, 2 and 3 respectively.

SINGLE-STAGE AXIAL TURBINE

The aerodynamic design of an axial turbine is very similar to the radial turbine, and can once again be designed by defining N, Ψ, and Φ. The axial velocity is assumed constant (*i.e.*, $c_{\mathrm{m2}} = c_{\mathrm{m3}}$), and since there is no change in the meanline radius between the inlet and outlet, there is no change in the blade velocity (*i.e.*, $u_2 = u_3$). However, unlike the radial turbine, the rotor outlet tangential velocity $c_{\theta 3}$ is not assumed to be zero. Therefore, to complete the design, the degree of reaction Λ is also defined as an input:

$$\Lambda = \frac{h_2 - h_3}{h_{02} - h_{03}}, \tag{4}$$

where h_2 and h_3 are the static enthalpies, and h_{02} and h_{03} are the total enthalpies at the rotor inlet and outlet respectively. Both the inlet and outlet conditions are taken at the rotor mid-span. It should be noted that a non-zero $c_{\theta 3}$ allows Ψ to be greater than 2, and that by defining Λ the rotor-outlet velocity triangle is fully defined and therefore the rotor outlet can be sized.

For the single-stage axial turbine design, another parametric investigation into the effects of the design parameters on the design of the turbine rotor can be conducted. For this investigation, the same stator loss coefficient of ζ_{n} = 0.075 is assumed. Referring to Fig. 3a, it is observed that, compared to radial turbines, axial turbines can achieve higher efficiencies at lower specific speeds. However, a preliminary study found that reducing the rotational speed reduced the maximum possible rotor-inlet blade height; for example, at 100 kRPM (ω_{s} = 0.16) the maximum blade height was only 1.6 mm. For this reason, the following analysis considers the same rotational speeds as the those considered for the radial turbine, namely 150, 200 and 250 kRPM.

Since the analysis of an axial turbine is very similar to a radial turbine, it can be inferred from the previous section that selecting the minimum allowable rotor diameter (d_2= 30 mm), and maximum absolute rotor-inlet flow angle (α_2= 82.5°), will result in the largest rotor-inlet blade height. Therefore, a parametric investigation into the effect of Λ on the turbine design, using these values has been conducted, and the results are presented in Fig. 6. To be consistent with the constraint applied to the rotor-inlet absolute flow angle, Λ is only varied between 0 and 0.5. This is because Λ > 0.5 corresponds to a rotor-outlet relative flow angle that is greater than the rotor-inlet absolute flow angle (*i.e.*, $\beta_3 > \alpha_2$), which would violate the maximum flow angle constraint (*i.e.*, β_3 > 82.5°).

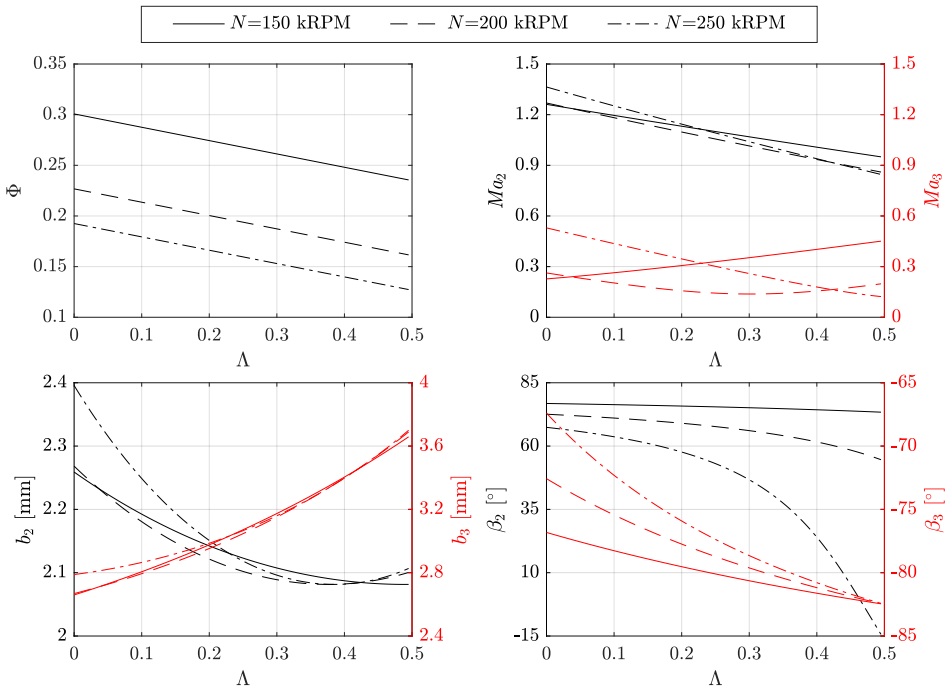

Figure 6. Effect of the degree of reaction Λ on the design of a single-stage axial turbine for different rotational speeds. Top-left: flow coefficient Φ; top-right: rotor inlet absolute Mach number Ma_2 and rotor outlet relative Mach number Ma_3; bottom-left: rotor inlet b_2 and rotor outlet b_2 blade heights; bottom-right: rotor inlet β_2 and rotor outlet β_3 relative flow angles.

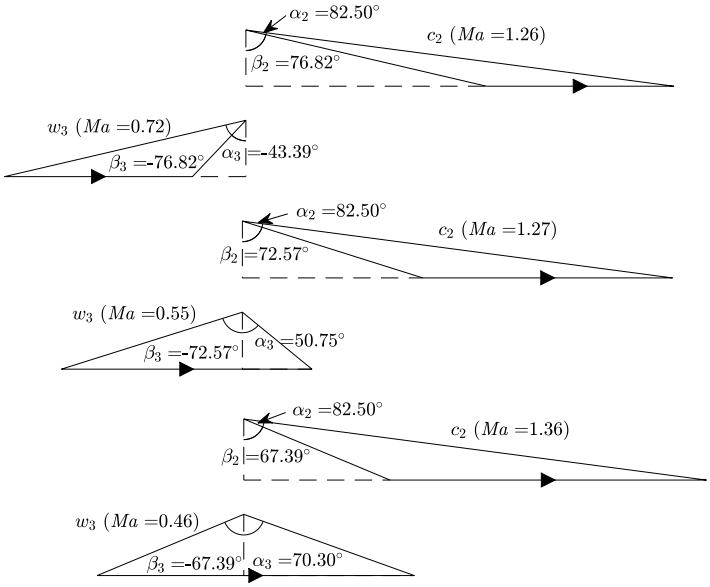

Figure 7. Rotor velocity triangles for the three single-stage axial turbine rotor designs. From top to bottom: design 1 (150 kRPM); design 2 (200 kRPM); design 3 (250 kRPM).

Table 3. Summary of single-stage axial turbine rotor designs that maximise the rotor-inlet blade height.

	N [kRPM]	Ψ	Φ	Λ	d_2 [mm]	b_2 [mm]	α_2 [°]	β_2, β_3 [°]	Ma_2
Axial-1 1	150	2.57	0.30	0.0	30.0	2.26	82.50	76.82	1.26
Axial-1 2	200	1.45	0.23	0.0	30.0	2.27	82.50	72.57	1.27
Axial-1 3	250	0.92	0.19	0.0	30.0	2.40	82.50	67.39	1.36

From Fig. 6 it is observed that for all three rotational speeds, a low degree of reaction is favourable to increase b_2. Unsurprisingly, the result of having the majority of the expansion within the stator is a high rotor-inlet Mach number, and a small change in volume through the rotor, resulting in a smaller rotor-outlet blade height compared to a higher degree of reaction. For each rotational speed, the design that maximises b_2 (*i.e.*, $\Lambda = 0$) is summarised in Tab. 3 and the velocity triangles are shown in Fig. 7. The stage loading coefficients are 2.57, 1.45 and 0.92 for the 150, 200 and 250 kRPM designs respectively. For the 200 and 250 kRPM rotational speeds, these are the same as for the radial turbine. For the 150 kRPM design, the stage loading for the axial turbine is higher than the radial turbine, owing to the non-zero value for $c_{\theta 3}$. It is also noted that $\Lambda = 0$ corresponds to $\beta_2 = \beta_3$, and this angle is reduced as the rotational speed is increased.

TWO-STAGE AXIAL TURBINE

For the two-stage axial turbine, the same procedure outlined for the single-stage axial turbine is applied. The only difference is that the total enthalpy drop is divided equally across the two-stages (*i.e.*, $\Delta h_{\text{stage}} = \Delta h_0/2$). Once the stage enthalpy drop is known, the process outlined in the previous section can be completed. For this preliminary design, the analysis is only applied to the first stage. This is because the volumetric flow rate through the machine increases as the pressure reduces. Therefore, the smallest blade dimensions will be at the rotor inlet of the first stage.

For the two-stage design, the same stator loss coefficient is assumed ($\zeta_{\text{n}} = 0.075$), and three rotational speeds are considered, namely 75, 125 and 175 kRPM, which correspond to first-stage specific speeds of 0.16, 0.26 and 0.37 respectively. Following on from the previous discussion regarding the single-stage axial turbine design, a preliminary study found that reducing the rotational speed below 75 kRPM resulted in very small rotor-inlet blade heights. Moreover, following from the analysis in the previous sections, it can again be stated that designs with the minimum rotor diameter ($d_2 \geq 30$ mm), and maximum absolute rotor-inlet flow angle ($\alpha_2 \leq 82.5°$) will correspond to the largest rotor-inlet blade heights. Therefore, another parametric investigation considering the effect of Λ on the rotor design can be completed. For brevity, the results from this analysis are not reported in this paper, but ultimately, it is observed that, unlike the single-stage axial turbine design, a high degree of reaction ($\Lambda = 0.5$) results in the largest rotor-inlet blade height. This is because in the two-stage turbine the enthalpy drop per stage is lower, and therefore the conditions at the rotor inlet remain subsonic for all values of Λ. However, in the single-stage design, the rotor inlet conditions are supersonic for $\Lambda < 0.35$ (Fig. 6). Since the mass flux (ρc) is always at a maximum at $Ma = 1$, the blade height can be maximised by increasing Λ for subsonic designs, and reducing Λ for supersonic designs. This also explains why b_2 increases for $\Lambda > 0.35$ in Fig. 6.

The final designs for the first-stage of a two-stage axial turbine are summarised in Tab. 3. It is noted that for the 75 kRPM design the rotor has a diameter of 39.26 mm, which is larger than the minimum diameter of 30 mm. This is because the stage-loading coefficient is capped at 3.0, in accordance with the range of values typically quoted within the literature (*i.e.*, the Smith chart [13]). The design of the second-stage is completed assuming the second stage has the same mid-span radius as the first stage, and that the flow coefficient, loading coefficient and degree of reaction are the same in both stages. This is considered to be a reasonable assumption for the preliminary design phase, since the second-stage will always have a larger blade height and is only of secondary interest. However, this assumption should be refined during future studies.

Table 3. Summary of the two-stage axial-turbine rotor designs that maximise the rotor-inlet blade height for the three different rotational speeds considered. The results reported correspond to the first stage.

	N [kRPM]	Ψ	Φ	Λ	d_2 [mm]	b_2 [mm]	α_2 [°]	β_2, β_3 [°]	Ma_2
Axial-2 1	75	3.00	0.26	0.5	39.26	1.74	82.50	75.25	0.67
Axial-2 2	125	1.85	0.19	0.5	30.00	2.40	82.50	66.17	0.61
Axial-2 3	175	0.94	0.13	0.5	30.00	2.47	82.50	–12.44	0.58

COMPARISON OF THE DIFFERENT TURBINE ARCHITECTURES

In the previous sections, three preliminary designs have been obtained for three different turbine architectures, namely radial, single-stage axial and two-stage axial turbines. In Fig. 8, the nine preliminary turbine designs are shown, as viewed from the meridional plane. For all three architectures, it is found that the maximum rotor-inlet blade height increases as the rotational speed is increased. Moreover, to ensure the rotor diameter is greater than 30 mm, the stage-loading coefficient must reduce, and this is also accompanied by a reduction in the flow coefficient. Comparing the different architectures, it is observed that the single-stage axial turbine design can facilitate a slightly larger blade height than a radial turbine rotating at the same speed. The blade height can be further increased by moving to a two-stage design, and reducing the rotational speed. It is also found that when moving from a single-stage axial design to a two-stage axial design, the degree of reaction changes. More specifically, for the single-stage turbine a zero reaction (impulse type) design should be selected, whilst the degree of reaction should be increased to 0.5 for the two-stage design.

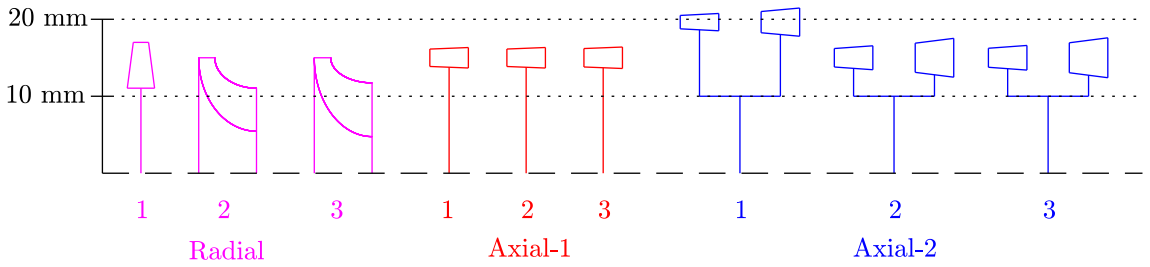

Figure 8. Comparison between the nine preliminary rotor designs. For the Radial/Axial-1 turbines '1', '2' and '3' correspond to rotational speeds of 150, 200 and 250 kRPM respective. For Axial-2 '1', '2' and '3' correspond to rotational speeds of 75, 125 and 175 kRPM respectively.

Ultimately, from Fig. 8 it can be observed that most of the designs all have similar dimensions, with an inlet diameter of 30 mm, and an inlet blade height around 2 mm. With a rotor this small, it is expected that all of the rotor designs will experience relatively large clearance losses, and increased viscous losses. Unfortunately, existing loss correlations for predicting turbine performance are not validated for sCO_2 applications. Therefore, the next stage of this research will require 3D CFD studies of the nine turbine designs shown in Fig. 8 to assess the aerodynamic performance that can be achieved by each design.

MECHANICAL AND ELECTRICAL DESIGN CONSIDERATIONS

The challenging operating conditions of a sCO_2 cycle mean that alongside considering the aerodynamic design of the turbine, the mechanical and electrical design must also be considered during the turbine design phase. This includes decisions such as choosing whether a hermetic turbine-generator assembly is used, which can be subject to high windage losses owing to the high density, or whether an external generator is used, in which case suitable shaft seals are required. Moreover, for a directly-coupled turbine and generator, expensive power electronics are required to match the grid frequency, or alternatively a gearbox with a high gear ratio is required. However, these challenges, despite their importance, pertain to any turbine architecture at the given scale.

Of more relevance when comparing different turbine architectures are factors such as the rotor-dynamics, axial thrust generated by the rotor and the blade stresses. For example, due to the high power density and high pressure, the stresses on the rotor blade may be too large to use a radial-inflow turbine with a non-zero blade angle, as in the case for Radial-2 design. Alternatively, due to the moderate tip speed, which ranges between 235 and 392 m/s for the single-stage turbine designs, means that shrouded rotors may be considered to improve aerodynamic performance, but may have consequences in terms of the rotor-dynamics of the shaft. Ultimately, these effects are hard compare at the preliminary level that is applied within this paper, and can only be compared after more detailed simulations are carried out. Therefore, an important next step in this research is to conduct rotor-dynamic and FEA simulations of the nine turbine designs identified, in addition to the already mentioned CFD simulations, to allow for a more detailed comparison. Moreover, it will be necessary to consider different bearing-shaft arrangements for

each design, in addition to giving consideration to the thermal management of the assembly to ensure suitable cooling is available for the bearings and high-speed generator [17].

CONCLUSIONS

In this paper, the design of the turbine for a small-scale (100 kW) supercritical CO_2 Rankine cycle with a turbine inlet temperature of 650 °C has been evaluated. To identify the most suitable designs, design models for radial-inflow, and single- and two-stage axial turbines have been developed, which use, as inputs, the loading coefficient, flow coefficient, and degree of reaction. The objective of the design study is to identify turbine designs that result in feasible blade heights. It is found that to obtain optimal efficiencies, a single-stage turbine must rotate at speeds in excess of a few hundred kRPM, and for the three different turbine architectures considered the resulting turbine has a diameter of 30 mm, and a minimum rotor blade height in the range of 1.74 to 2.47 mm. More generally, it is found that to obtain a feasible blade height, it is necessary to design the turbine with a high loading coefficient, and low flow coefficient, corresponding to a high absolute flow angle. Moreover, when considering axial turbines, an impulse-type turbine, with a low degree of reaction, is most suitable for a single-stage design, and this results in supersonic conditions at the rotor inlet. On the other hand, for a two-stage axial turbine, a higher degree of reaction is more suitable, whilst conditions at the rotor inlet remain subsonic.

REFERENCES

[1] Dostal, V., 2004, “A supercritical carbon dioxide cycle for next generation nuclear reactors”, PhD Thesis, Massachusetts Institute of Technology, Boston, USA.

[2] Garg, P., Kumar, P., Srinivasan, K., 2013, “Supercritical carbon dioxide Brayton cycle for concentrated solar power”, Journal of Supercritical Fluids, 76, pp. 54-60.

[3] Moullec, Y. L., 2013, “Conceptual study of a high efficiency coal-fired power plant with CO_2 capture using a supercritical CO_2 Brayton cycle”, Energy, 49, pp. 32-46.

[4] Bianchi, G., Tassou, S.A., Ge, Y., Jouhara, H., Tasmos, K., Leroux, A., de Miol, M., 2016, “Design considerations on a small scale supercritical CO2 power system for industrial high temperature waste heat to power applications”, 1st European Seminar on Supercritical CO_2 (sCO_2) Power Systems, 29-30th September, Vienna, Austria.

[5] Moore, J., Brun, K., Evans, N., Kalra, C., 2015, “Development of a 1 MWe supercritical CO_2 test loop”, Proceedings of ASME Turbo Expo 2015: Turbine Technical Conference and Exposition, 15-19th June, Montreal, Canda, GT2015-43771.

[6] Held, T.J., 2014, “Initial test results of a megawatt-class supercritical CO_2 heat engine”, The 4th International Symposium on Supercritical CO2 Power Cycles, 9-10th September, Pittsburgh, USA.

[7] Cho, J., Choi, M., Baik, Y-J., Lee, G., Ra, H-S., Kim, B., Kim, M., 2016, “Development of the turbomachinery for the supercritical carbon dioxide power cycle”, International Journal of Energy Research, 40, pp. 587-599.

[8] Wright, S.A., Radel, R.F., Vernon, M.E., Rochau, G.E., Pickard, P.S., 2010, “Operation and analysis of a supercritical CO_2 Brayton cycle”, Sandia Report SAND2010-0171, Sandia National Laboratories, Albuquerque, NM.

[9] Kimball, K.J., Rahner, K.D., Nehrbauer, J.P., Clementoni, E.M., 2013, “Supercritical carbon dioxide Brayton cycle development overview”, Proceedings of ASME Turbo Expo 2013: Turbine Technical Conference and Exposition, 3-7th June, San Antonio, USA.

[10] Crespi, F., Gavagnin, G., Sánchez, D., Martínez, G.S., 2017, “Supercritical carbon dioxide cycles for power generation: A review”, Applied Energy, 195, pp. 152-183.

[11] Invernizzi, C.M., van der Stelt, T., 2012, “Supercritical and real gas Brayton cycles operating with mixtures of carbon dioxide and hydrocarbons”, Proceedings of the Institution of Mechanical Engineers Part A: Journal of Power and Energy, 226(5), pp. 682-693.

[12] Wright, S.A., Pickard, P.S., Vernon, M.E., Radel, R.F., 2013, “Enhancing power cycle efficiency for a supercritical Brayton cycle power system using tunable supercritical gas mixtures”, US Patent 20130033044A1.

[13] Dixon, S.L., Hall, C.A., 2013, *Fluid Mechanics and Thermodynamics of Turbomachinery*, 7th Ed., Butterworth-Heinemann, Oxford, UK.

[14] Lemmon, E.W., Huber, M.L., McLinden, M.O., 2013, “NIST Standard Reference Database 23: Reference Fluid Thermodynamic and Transport Properties-REFPROP”, Version 9.1, National Institute of Standards and Technology, Standard Reference Data Program, Gaithersburg, USA.

[15] Costall, A.W., Hernandez, A.G., Newton, P.J., Marinez-Botas, R.F., 2015, “Design methodology for radial turbo expander in mobile organic Rankine cycle applications”, Applied Energy, 157, pp. 729-743.
[16] Rahbar, K., Mahmoud, S., Al-Dadah, R.K., Moazami, N., 2015, “Modelling and optimization of organic Rankine cycle based on a small-scale radial inflow turbine”, Energy Conversion and Management, 91, pp. 186-198.
[17] Arroyo, A., McLorn, M. Fabian, M., White, M. Sayma, A.I., 2016, “Rotor-dynamics of different shaft configurations for a 6 kW micro gas turbine for concentrated solar power”, Proceedings of the ASME Turbo Expo 2016: Turbomachinery Technical Conference and Exposition, 13-17th June, Seoul, South Korea.

NOMENCLATURE

α	absolute flow angle, °
β	relative flow angle, °
ϵ_{r}	recuperator effectiveness
ζ_{n}	stator loss coefficient
η	efficiency
Λ	degree of reaction
Φ	flow coefficient
Ψ	blade-loading coefficient
ω	rotational speed, rad/s
ω_{s}	specific speed, rad/s
b	blade height, m
c	absolute velocity, m/s
d	diameter, m
h	enthalpy, J/kg
$\dot{m}$	mass-flow rate, kg/s
$\dot{W}$	power, J/s
$\dot{V}$	volumetric-flow rate, m^3/s
Ma	Mach number
N	rotational speed, RPM
p	pressure, Pa
PR	pressure ratio
T	temperature, K
u	blade velocity, m/s
w	relative velocity, m/s
Δh_0	stage enthalpy drop, J/kg
Δh_{ss}	isentropic enthalpy drop, J/kg

Subscripts

θ	tangential
0	total conditions
1	turbine inlet
2	rotor inlet
3	rotor outlet
c	compression process inlet/compressor
is	isentropic
m	meridional
p	polytropic
th	thermal

BIOGRAPHY

Dr Martin White is a Research Associate within the Turbomachinery and Energy Systems research group at City, University of London. He obtained his PhD from City in October 2015, and his MEng in Mechanical Engineering from the University of Southampton in 2015. His primary interest is in understanding and characterising the performance of turbomachines accounting for real-gas effects.

Professor Abdulnaser Sayma is a Professor of Energy Engineering, at City, University of London since 2013, and the leader of the Turbomachinery and Energy Systems research group. He obtained his PhD from the University of Manchester in 1994 and worked as a Rolls Royce research fellow at Imperial College London before becoming a professor of CFD at University of Sussex in 2006. His main research area is the development of compressible flow CFD methods for turbomachinery applications and the development of turbo compressors and expanders with current emphasis on micro-gas turbines and organic Rankine cycles. He has been leading a team developing a micro-gas turbine powered by concentrated solar power using a solar dish system (OMSoP), and currently leads the SolGATS project for integrating solar powered micro-gas turbines with thermal-energy storage. He is also leading EPSRC funded research on fundamental studies on organic Rankine cycle expanders (NextORC).